

DNA binding property, nuclease activity and cytotoxicity of Zn(II) complexes of terpyridine derivatives

Qin Jiang · Jianhui Zhu · Yangmiao Zhang ·
Nan Xiao · Zijian Guo

Received: 11 April 2008 / Accepted: 30 September 2008 / Published online: 18 October 2008
© Springer Science+Business Media, LLC. 2008

Abstract Two zinc(II) terpyridine complexes $\text{Zn}(\text{atpy})_2(\text{PF}_6)_2$ (**1**) ($\text{atpy} = 4'\text{-p-N}9'\text{-adeninylmethylphenyl-2,2':6,2''-terpyridine}$) and $\text{Zn}(\text{ttpy})_2(\text{PF}_6)_2$ (**2**) ($\text{ttpy} = 4'\text{-p-tolyl-2,2':6,2''-terpyridine}$) have been synthesized and characterized by elemental analysis, ^1H NMR and electrospray mass spectroscopy. The structure of complex **2** was also determined by X-ray crystallography, which revealed a ZnN_6 coordination in an octahedral geometry with two terpyridine acting as equatorial ligands. The circular dichroism data showed that complex **1** exhibited an ICD signal at around 300 nm and induced more evident disturbances on DNA base stacking than complex **2**, reflecting the impact of the adenine moiety on DNA binding modes. Complex **1** exhibited higher cleavage activity to supercoiled pUC 19 DNA than complex **2** under aerobic conditions, suggesting a promotional effect of adenine moiety in DNA nuclease ability. Interestingly, both complexes demonstrated potent in

vitro cytotoxicity against a series human tumor cell lines such as human cervix carcinoma cell line (HeLa), human liver carcinoma cell line (HepG2), human galactophore carcinoma cell line (MCF-7) and human prostate carcinoma cell line (pc-3). The cytotoxicity is averagely 10 times more active than the anticancer drug cisplatin.

Keywords Adenine · DNA binding · DNA cleavage · Terpyridine · Zinc

Introduction

DNA binding and cleavage are two critical events for gene mutation and carcinogenesis in biological systems (Haq and Ladbury 2000). Therefore, DNA-targeting reagents may have great prospects as artificial nucleases, DNA structural probes or gene-selective drugs (Hannon 2007). Metal complexes have been studied extensively due to their diversity in structure and reactivity (Jiang et al. 2007). For example, metalated terpyridine complexes are well documented for their high DNA affinity through intercalation (Glover et al. 2003; Lavin et al. 2005), DNA nuclease activity (Szaciłowski et al. 2005; Holder et al. 2004) and cytotoxicity (Li et al. 2006; Novakova et al. 1995).

Recent reports showed that small molecules containing nucleobases exhibited interesting recognition ability to the complementary base in single or double

Electronic supplementary material The online version of this article (doi:10.1007/s10534-008-9166-3) contains supplementary material, which is available to authorized users.

Q. Jiang
Chemistry Department, Huaihai Institute of Technology,
Lianyungang 222005, People's Republic of China

Q. Jiang · J. Zhu · Y. Zhang · N. Xiao · Z. Guo (✉)
State Key Laboratory of Coordination Chemistry, Nanjing
University, Nanjing 210093, People's Republic of China
e-mail: zgao@nju.edu.cn

stranded polynucleotides (Tumir et al. 2003, 2005; Juranović et al. 2002). Especially, an acridine-phenanthridinium-adenine conjugate was particularly promising since it generated promising double-stranded DNA cleavage in a selective way, and the cleavage is achieved via its intrinsic β -elimination cleaving activity on the a basic strand and its radicalar cleavage activity on the opposite strand (Martelli et al. 2002). Therefore, nucleotide recognition has been utilized to promote irreparable multiple DNA damage. Another interesting example is that copper-metalated adenine-containing polymers were found to promote the hydrolysis of natural phosphate esters in a highly efficient and catalytic fashion, possibly due to the synergia between adenine and copper ions (Srivatsan et al. 2002).

To continue our investigations on the structure-activity relationship of metal terpyridine complexes (Shi et al. 2006; Jiang et al. 2008), in this work we report the synthesis and characterization of two zinc complexes $\text{Zn}(\text{atpy})_2(\text{PF}_6)_2$ (**1**) and $\text{Zn}(\text{ttpy})_2(\text{PF}_6)_2$ (**2**), in which atpy contains a nucleobase adenine. The DNA binding ability, DNA nuclease activity and in vitro cytotoxicity of both complexes were studied and compared in order to illustrate the role of adenine moiety in improving the bioactivity of complex **1**.

Experimental

Materials and physical measurements

Reagents such as methanol, ethanol, acetone, anhydrous DMF, $\text{Zn}(\text{NO}_3)_2 \cdot 3\text{H}_2\text{O}$ were of analytical grade and were used without further purification. The 4'-p-tolyl-2,2':6,2''-terpyridine, 4'-p-bromomethylphenyl -2,2':6,2''-terpyridine were prepared according to the reported procedures (Neve et al. 1999; Johansson et al. 2003). The ligand 4'-p-N9'-adeninylmethylphenyl-2,2':6,2''-terpyridine (atpy) was obtained by the reaction of the adenine with 4'-p-bromomethylphenyl -2,2':6,2''-terpyridine (Jiang et al. 2008). The pUC19 plasmid DNA was purchased from TaKaRa Biotechnology (Dalian). The electrospray mass spectra were recorded using an LCQ electron spray mass spectrometer (ESMS, Finnigan) and Isopro 3.0 was used to simulate the isotopic distribution patterns of the assigned ions. The ^1H NMR data were carried out on a 500 MHz Bruker

DMX spectrometer. The elemental analysis was performed on a Perkin-Elmer 240C analytical instrument.

Syntheses

4'-p-tolyl-2,2':6,2''-terpyridine (ttpy)

A mixture of 2-acetylpyridine (3 ml, 0.026 mol), 3 ml, 0.025 mol 4-methylbenzaldehyde (3 ml, 0.025 mol) and 100 ml aqueous solution of 2% NaOH were stirred at 25°C for 8 h, then 18 g solid NaOH and 3 ml 2-acetylpyridine were added to the mixture to get a red solution. After the solution was heated at 70°C for 8 h, it was cooled and dark solid were obtained, which was then dissolved in 200 ml ethanol to get a clear red solution. Then 18 g $\text{CH}_3\text{COONH}_4$ was added in three portions under reflux in 3 h. The hot solution was filtered and the filtrate was left to crystallize at room temperature. The yellow needle crystals were collected and dried in vacuum. Yield: 3.8 g, 47%. M.p. 166°C. ^1H NMR (500 MHz, d_6 -DMSO, 25°C, TMS): 8.75 (t, 2H, $\text{H}_{6,6''}$), 8.66 (m, 4H, $\text{H}_{3,5''} + \text{H}_{3,3''}$), 8.02 (m, 2H, $\text{H}_{4,4'}$), 7.81 (d, 2H, benzene-H, $J = 7.85$), 7.51 (m, 2H, $\text{H}_{5,5''}$), 7.39 (d, 2H, benzene-H, $J = 7.5$), 2.39 (s, 3H, methyl-H). ES-MS (m/z , positive mode): 324.3 $[\text{LH}]^+$, 351.3 $[\text{Na}(\text{CH}_3\text{OH})\text{L}_2\text{H}]^{2+}$, 669.0 $[\text{NaL}_2]^+$.

4'-p-N9'-adeninylmethylphenyl-2,2':6,2''-terpyridine (atpy)

Adenine (0.135 g, 1 mmol), sodium hydride (0.048 g, 2 mmol) and 4'-p-bromomethylphenyl -2,2':6,2''-terpyridine (0.402 g, 1 mmol) were subsequently added to an anhydrous DMF (20 ml). The mixture was stirred at 80°C under dinitrogen for 12 h and then the solvent was evaporated under reduced pressure. The residue was then recrystallized from ethanol to give atpy as a white solid. Yield: 0.313 g, 68.7%. M.p. 185°C. ^1H NMR (500 MHz, d_6 -DMSO, 25°C, TMS): $\delta = 8.72$ (s, 2H; $\text{H}_{6,6''}$), 8.61 (d, 4H; $\text{H}_{3,5''} + \text{H}_{3,3''}$), 8.31 (s, 1H; C8'-purine-H), 8.16 (s, 1H; C2'-purine-H), 7.98 (t, 2H; $\text{H}_{4,4''}$; $J = 7.4$ Hz), 7.87 (d, 2H; benzene-H, $J = 7.6$ Hz), 7.48 (d, 4H; $\text{H}_{5,5''} + \text{benzene-H}$), 7.25 (s, 2H; NH_2), 5.47 (s, 2H; methylene-H). ES-MS (m/z , positive mode): 457.2 $[\text{LH}]^+$.

Zn(atpy)₂(PF₆)₂ (1)

A mixture of Zn(NO₃)₂ · 6H₂O (0.149 g, 0.5 mmol) and atpy (0.456 g, 1 mmol) in a mixture of ethanol and water (50 ml) was stirred for 12 h at 30°C, then KPF₆ (0.184 g, 1 mmol) was added. The solids were filtered and washed with acetone and diethyl ether, and dried in air. Yield: 0.363 g, 57.4%. M.p. >300°C. ¹H NMR (500 MHz, d₆-DMSO, 25°C, TMS): δ = 9.32 (s, 4H, H_{6'}), 9.08 (d, 4H, H_{3,3'}, *J* = 7.5 Hz), 8.41 (s, 2H, C8'-purine-H), 8.36 (d, 4H, H_{3,5'}, *J* = 7.5 Hz), 8.26 (t, 4H, H_{4,4'}, *J* = 7.25 Hz), 8.21 (s, 2H, C2'-purine-H), 7.92 (d, 4H, benzene-H, *J* = 3.5 Hz), 7.69 (d, 4H, H_{5,5'}, *J* = 8.0 Hz), 7.47 (t, 4H, benzene-H, *J* = 5.5 Hz), 5.58 (s, 4H, methylene-H). ES-MS (*m/z*, positive mode): 488.3, [Zn(atpy)₂]²⁺; elemental analysis calcd (%) for C₅₄H₄₀F₁₂N₁₆P₂Zn (1267): C 51.14, H 3.16, N 17.68; found: C 50.78, H 4.09, N 17.71.

Zn(tpy)₂(PF₆)₂ (2)

A mixture of Zn(NO₃)₂ · 6H₂O (0.149 g, 0.5 mmol) and tpy (0.323 g, 1 mmol) in a mixture of ethanol and water (50 ml) was stirred for 12 h at 30°C, then KPF₆ (0.184 g, 1 mmol) was added. The solids were filtered and washed with acetone and diethyl ether, and dried in air. Yellow crystals suitable for X-ray diffraction were obtained by vapor diffusion of diethyl ether into a solution of the solid in the CH₃CN. Yield: 0.282 g, 56.3%. M.p. >300°C. ¹H NMR (500 MHz, d₆-DMSO, 25°C, TMS): δ = 9.38 (s, 4H, H_{6'}), 9.17 (d, 4H, H_{3,3'}, *J* = 7.7 Hz), 8.39 (d, 4H, H_{3,5'}, *J* = 7.2 Hz), 8.29 (t, 4H, H_{4,4'}, *J* = 7.15 Hz), 7.96 (s, 4H, benzene-H), 7.60 (d, 4H, H_{5,5'}, *J* = 7.25 Hz), 7.50 (s, 4H, benzene-H); 2.37 (s, 3H, methyl-H). ES-MS (*m/z*, positive mode): 355.5, [Zn(tpy)₂]²⁺; 854.7, {[Zn(tpy)₂](PF₆)}⁺ elemental analysis calcd (%) for C₄₄H₃₄F₁₂N₆P₂Zn (1002.1): C 52.74, H 3.42, N 8.38; found: C 52.57, H 3.53, N 8.39.

X-ray crystallography

For Zn(tpy)₂(PF₆)₂, a single crystal of the complex was mounted on a glass fiber. Intensity data were collected at 298 K on a Bruker SMART CCD area detector diffractometer operating in the $\phi - \omega$ scan mode with graphite-monochromated MoK α radiation

($\lambda = 0.71073$ Å). Empirical absorption corrections were carried out using a multiscan program. The SMART software was used for data acquisition and the SAINT software for data extraction. Absorption correction was made using SADABS (Sheldrick 2001). The structures were solved by direct methods and refined on *F*² by fullmatrix least-squares methods by using the SHELXTL program (Sheldrick 1997). All non-hydrogen atoms were refined anisotropically. The hydrogen atoms of the complex were located from the difference Fourier maps and refined isotropically. The data collection and refinement parameters of Zn(tpy)₂(PF₆)₂ are given in Table 1. The crystallographic data are deposited in Cambridge Crystallographic Data Center with a registration number of 615623. These data can be obtained free of charge from the Cambridge Crystallographic Data Center via http://www.ccdc.cam.ac.uk/data_request/cif.

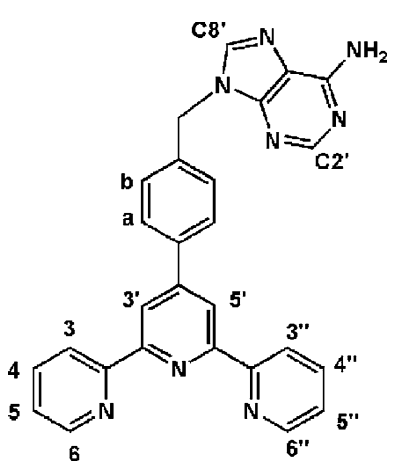
DNA binding and cleavage experiments

The CD spectra of DNA was recorded on a Jasco J-810 automatic recording spectropolarimeter at room temperature at increasing complex/DNA ratio (*r* = 0.0, 0.2, 0.4). Each sample solution was scanned in the range of 420–220 nm at a speed of 10 nm min^{−1} and the buffer background was automatically subtracted. The concentration of DNA was 1.0 × 10^{−4} M.

The DNA cleavage activity of complexes **1** and **2** was studied by agarose gel electrophoresis. Supercoiled pUC19 DNA (200 ng) in Tris–HCl buffer (50 mM) containing 50 mM NaCl (pH 7.4) was treated with copper complexes to yield a total volume of 10 µl and then incubated in dark for 12 h at 37°C. The reaction was quenched by the addition of 1 µl loading buffer, and then the resulting solutions were loaded on a 0.7% agarose gel. Electrophoresis was carried out at 50 V for 2 h in TAE buffer (40 mM Tris acetate/1 mM EDTA). DNA bands were visualized under UV light and photographed. The quantification of each form of DNA was made by densitometric analysis of ethidium bromide containing agarose gel. A correction factor of 1.47 was used for supercoiled DNA (form I) taking into account the weaker intercalation of EB to SC compared to nicked (form II) and linear DNA (form III).

Table 1 The ^1H NMR spectral data of ttpy, atpy and their Zn(II) complexes **1** and **2**

	ttpy		atpy		$\text{Zn}(\text{atpy})_2(\text{PF}_6)_2$		$\text{Zn}(\text{ttpy})_2(\text{PF}_6)_2$	
	δ (ppm)	J (Hz)	δ (ppm)	J (Hz)	δ (ppm)	J (Hz)	δ (ppm)	J (Hz)



CH_2/CH_3
 NH_2
 H_b
 $\text{H}_{5,5''}$
 H_a
 $\text{H}_{4,4''}$
 $\text{C}2'\text{-purine-H}$
 $\text{C}8'\text{-purine-H}$
 $\text{H}_{3',5'}$
 $\text{H}_{3,3''}$
 $\text{H}_{6,6''}$

CH_2/CH_3	2.39		5.46		5.58		2.37	
NH_2			7.25					
H_b	7.39	7.5	7.48		7.47	5.5	7.50	
$\text{H}_{5,5''}$	7.51		7.49		7.69	8.0	7.60	7.25
H_a	7.81	7.85	7.88	7.6	7.92	3.5	7.96	
$\text{H}_{4,4''}$	8.01		7.99	7.4	8.26	7.25	8.29	7.15
$\text{C}2'\text{-purine-H}$			8.16		8.21			
$\text{C}8'\text{-purine-H}$			8.31		8.41			
$\text{H}_{3',5'}$	8.66		8.61		8.36	7.5	8.39	7.2
$\text{H}_{3,3''}$	8.74		8.64		9.08	7.5	9.17	7.7
$\text{H}_{6,6''}$	8.75		8.71		9.32		9.38	

Cytotoxicity assay

The human cell lines HeLa, pc-3 and MCF-7 were maintained in DMEM. HepG2 cells were maintained in RPMI 1640 medium. All media were supplemented with newborn calf serum (10%). Cultures were incubated at 37°C in a humidified atmosphere of 5% CO_2 /95% air. All cultures were daily passaged. Assays of cytotoxicity were conducted in 96-well, flat-bottomed microtitre plates. The supplemented culture medium (50 μl) with cells (1×10^5 cells per ml) was added to the wells. Compounds were dissolved in DMSO and diluted in the culture medium with the final concentrations of 2–200 μM , and the solutions were added to the wells with 50 μl each well. The microtitre plates were incubated at 37°C in a humidified atmosphere of 5% CO_2 /95% air

for 48 h. All the assays were run in parallel with a negative and a positive control, in which cisplatin was used as a cytotoxic agent. The evaluation of cytotoxicity was carried out using a modified method of MTT assay. About 10 μl MTT solution with a concentration of 4 mg/ml were added into each well, and after 2 h incubation at 37°C in a humidified atmosphere of 5% CO_2 /95% air, a water solution containing 10% w/v of SDS and 50% v/v of DMF was added into each well to lyse the cells and to solubilize the formazan complex formed. After 20 h incubation, the OD value was measured by using a microtitre plate reader at 570 nm and the percentages of cell survival were determined. The cytotoxicity was evaluated based on the percentage cell survival in a dose-dependent manner relative to the negative control.

Results and discussion

Synthesis and characterization

The synthetic procedure of complexes **1** and **2** is shown in Scheme 1.

Two zinc(II) complexes were prepared by direct reaction of the corresponding ligands with $\text{Zn}(\text{NO}_3)_2 \cdot 6\text{H}_2\text{O}$ in ethanol in relative good yield, respectively. The target complexes were obtained by precipitation using KPF_6 . In the electrospray ionization mass (ESI-MS) spectra for the two complex, the signals 488.3, 355.2, and 854.7 were attributed to $[\text{Zn}(\text{atpy})_2]^{2+}$, $[\text{Zn}(\text{ttpy})_2]^{2+}$ and $[\text{Zn}(\text{ttpy})_2(\text{PF}_6)]^+$, respectively, (Figs. S1, S2). Their isotopic distribution patterns are almost identical to the corresponding simulated ones given by Isopro 3.0.

The ^1H NMR spectra of both Zn(II) complexes are shown in Figs. S3 and S4. The proton chemical shifts are shown in Table 1, which are assigned with the aid of the corresponding simulated ones given by ACD/HNMR 2.0 and comparison with those of corresponding ligands and similar compounds (Shi et al. 2006; Jiang et al. 2008). The ^1H NMR data showed the proton resonances of H3,3'' and H6,6'' of the terpyridine moiety in both complexes located at 9.38–9.08 ppm, which are significantly shifted to downfield

compared to the signals in free ligands at 8.64–8.75 ppm. Together with the 0.3 ppm shift to upfield of the proton resonances of H3',5', these data suggest the coordination of terpyridine moiety to Zn(II) center by {N, N, N} mode. For complex **1**, the proton signals for adenine and methylene groups (8.41, 8.21 and 5.58 ppm, respectively) are similar to those for free atpy (8.31, 8.16 and 5.46 ppm), indicating that the adenine moiety is not involved in Zn(II) coordination.

Crystal structure of complex **2**

As shown in Fig. 1, complex **2** is ionic, presenting a $[\text{Zn}(\text{ttpy})_2]^{2+}$ cationic core. Two ttpy act as equatorial ligands in a double-tridentate mode. The {N, N, N} coordination planes are nearly perpendicular to each other with the dihedral angles of about 84.5° . The coordination distance of $\text{Zn}-\text{N}_{\text{lateral}}$ ($\text{Zn}(1)-\text{N}(1)$, 2.170(2) Å) is slightly longer than that of $\text{Zn}-\text{N}_{\text{central}}$ ($\text{Zn}(1)-\text{N}(2)$, 2.068(3) Å), which is comparable with those found in similar zinc(II) terpyridine complexes (Harvey et al. 2004). Nonclassical hydrogen bond $\text{C4B}\cdots\text{F3A}$ was found between $[\text{Zn}(\text{ttpy})_2]^{2+}$ cationic core and anionic PF_6^- (Steiner 1996), and the bond length is 2.48 Å, which benefit the formation of a 3D cationic network in the crystal packing of complex **2** (Fig. 2).

Scheme 1 Preparation of complexes **1** and **2**

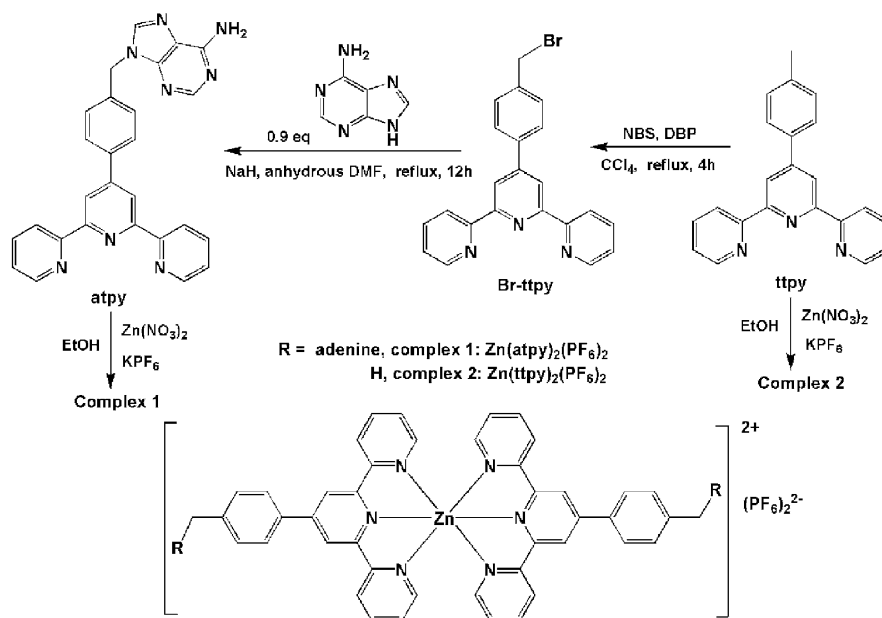


Fig. 1 Crystal structure of $\text{Zn}(\text{ttpy})_2(\text{PF}_6)_2$ (the hydrogen bond $\text{C4B}\cdots\text{F3A}$ was labeled, and the bond length is 2.48 Å)

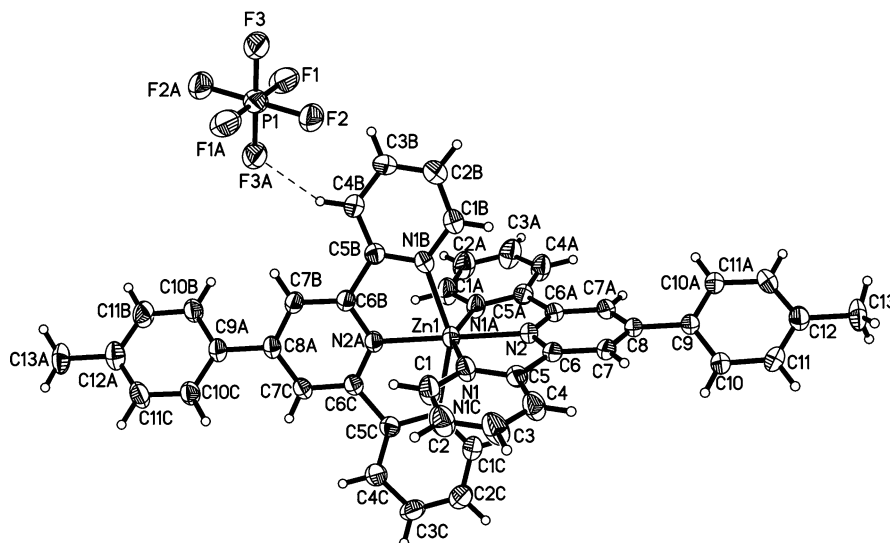
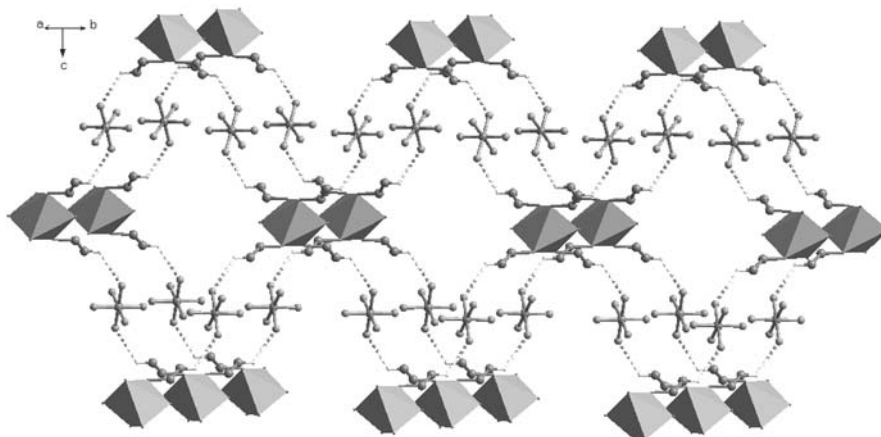


Fig. 2 The 3D net structure of $\text{Zn}(\text{ttpy})_2(\text{PF}_6)_2$ linked by $\text{C4}\cdots\text{H4}\cdots\text{F3}$ (only the center zinc, six nitrogen atom, C4, C5, H4 together with PF_6^- left for clarity and the polyhedron represents the $[\text{Zn}(\text{ttpy})_2]^{2+}$)



DNA binding ability

The DNA binding ability of both complexes was studied by CD spectrum using pUC19 DNA as substrate. The CD spectrum of plasmid DNA (pUC 19, supercoiled) showed a positive band at 268 nm due to base-stacking and a negative band at 244 nm due to the right-handed helicity. Both bands are quite sensitive to the interaction mode with small molecules (Nejedlý et al. 2005). As shown in Fig. 3a and b, the positive band (~ 268 nm) decreased significantly in intensity while the negative band (~ 268 nm) decreased only slightly in intensity with the increase of the complex concentration, suggesting that both complexes induce more evident disturbance on DNA base stacking than on DNA right-handed

helicity. Larger intensity decrease in the DNA CD spectra was observed for complex **1** (38.6%) than for complex **2** (19.7%), indicating the former exerts more effective perturbation than the latter on tertiary structure of DNA. It is worthy to note that a positive ICD band appeared in the region of 290–360 nm when the complex **1** was added into DNA. The ICD signal gave $\Delta\epsilon$ values of less than 10 units (Fig. 4), consistent with DNA intercalation (Berova et al. 2000). However, no such an ICD signal was observed in complex **2** and DNA system. Therefore, the adenine moiety in complex **1** can intercalate into the DNA base pairs and induce more evident disturbance on DNA conformation. Similar effect was observed in copper complexes of the same ligands (Jiang et al. 2008).

Fig. 3 CD spectra of supercoiled plasmid DNA (1×10^{-4} M, pUC19) in the absence and presence of $\text{Zn}(\text{atpy})_2(\text{PF}_6)_2$ or $\text{Zn}(\text{ttpy})_2(\text{PF}_6)_2$ at r ($[\text{Complex}]/[\text{DNA}]$) of 0.2 and 0.4: **a** plasmid DNA with $\text{Zn}(\text{atpy})_2(\text{PF}_6)_2$; **b** plasmid DNA with $\text{Zn}(\text{ttpy})_2(\text{PF}_6)_2$

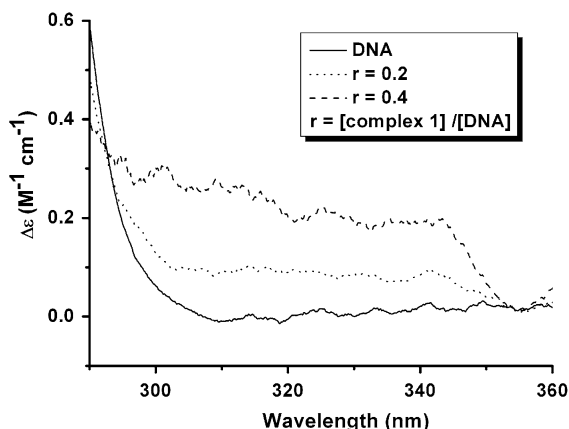
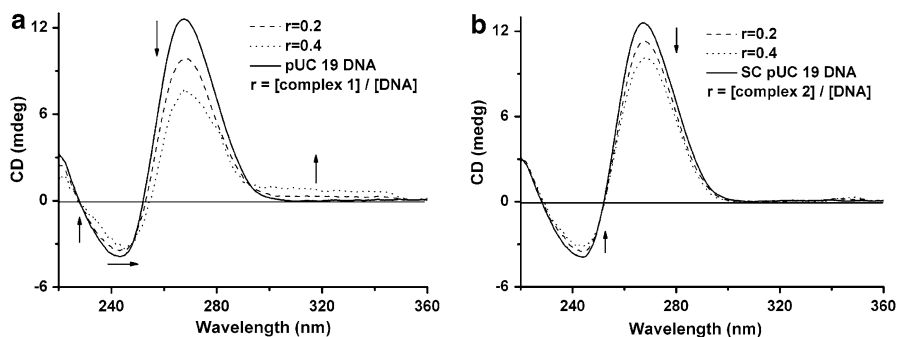


Fig. 4 The ICD band of the complex **1** when added into plasmid DNA (1×10^{-4} M, pUC19)

DNA nuclease activity

The DNA cleavage activities of complexes **1** and **2** have been studied under physiological pH and temperature by gel electrophoresis using supercoiled pUC19 plasmid DNA as substrate. Figure 5 shows the results obtained with complexes of different concentration in 50 mM Tris–HCl/50 mM NaCl buffer (pH 7.4) at 37°C in 12 h, which indicates that the chemical nuclease ability follows the order of complex **1** > complex **2**. Complex **1** exhibited

double-stranded DNA cleavage ability when the complex concentration reached 60 μM , resulting 23% nicked (Form II) and 8% linear (Form III) DNA. However, complex **2** can only convert supercoiled (Form I) DNA to nicked DNA even at 80 μM (Fig. 5). Concerning the similarity in zinc coordination between complexes **1** and **2**, this difference in nuclease activity can be attributed to the promotional effect of the adenine moiety. Control experiments with two ligands atpy and ttpy were conducted, which showed that at a concentration of 100 μM atpy is inactive while ttpy can convert 25% supercoiled DNA into nicked DNA. This result again confirmed that the double-stranded cleavage activity of complex **1** arises from the whole complex while that of complex **2** comes mainly from the ttpy ligand.

In vitro cytotoxicity

There are scarce reports on the cytotoxicity of zinc complexes (Choi et al. 2004; Kovala-Demertzi et al. 2006). Two zinc(II)-phthalocyanines complexes were reported to exhibit photocytotoxicity towards murine macrophage cell line (J774), however, they are inactive towards human hepatocellular carcinoma cell line (HepG2) (Choi et al. 2004). Some other Zn(II) complexes of thiosemicarbazones displayed IC_{50} values in a μM range against several human and

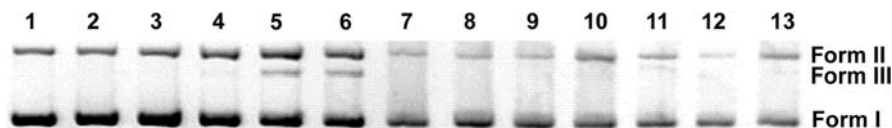


Fig. 5 Agarose gel electrophoresis patterns for the cleavage of pUC19 plasmid DNA (0.02 mg ml^{-1} , 30 μM base pair) by complex **1** and complex **2** in the dark for 12 h in Tris–HCl buffer (50 mM, pH 7.4) at 37°C: Lane 1, DNA control; lane

2–6, DNA + complex **1** (10, 20, 30, 60 and 80 μM); lane 7–11, DNA + complex **2** (10, 20, 30, 60 and 80 μM), lane 12, DNA + 100 μM atpy; Lane 13, DNA + 100 μM ttpy

Table 2 IC₅₀ values (μM) of complexes **1** and **2** for different human cancer cell lines

	MCF-7	HePG2	pc-3	HeLa
ttpy	1.71	^a	1.33	^a
atpy	18.4	^a	6.23	^a
Zn(atpy) ₂ (PF ₆) ₂	1.96	0.68	0.64	4.20
Zn(ttpy) ₂ (PF ₆) ₂	1.81	0.43	0.76	1.53
cisplatin	14.49	2.45	8.18	10.47

^a The cytotoxicity of the ligand against the selected cancer cell line does not depend on its dosage so that it is difficult to determine the accurate IC₅₀, see Fig. S5

mouse tumor cells, and their cytotoxicity was attributed to the ligands (Kovala-Demertzi et al. 2006).

In this work, we evaluated the in vitro cytotoxic activities of both zinc(II) complexes against four human tumor cell lines: HeLa, MCF-7, HepG2 and pc-3 cell lines. As shown in Table 2, both the two ligands and their zinc(II) complexes demonstrated higher in vitro cytotoxicity than cisplatin against selected tumor cell lines. Zn(atpy)₂(PF₆)₂ is much cytotoxic, with about 10 times higher than atpy against MCF-7 and pc-3 cell lines, indicating the crucial attribution of the metallization. However, the cytotoxicity of Zn(ttpy)₂(PF₆)₂ is much similar to that of ttpy, reflecting the important impact of the ligand. The cytotoxicity of two complexes follows the order: Zn(ttpy)₂(PF₆)₂ > Zn(atpy)₂(PF₆)₂, which is opposite to their order of DNA binding and DNA nuclease ability of the two complexes. Therefore events other than DNA binding and DNA damage could be responsible for the observed cytotoxicity of the complexes.

Conclusion

The comparison of DNA binding properties, nuclease activity and cytotoxicity of complexes **1** and **2** revealed that the biological effects induced by the incorporation of nucleobase adenine. Because of the presence of adenine moiety in complex **1**, more significant structural change of DNA and more effective DNA cleavage activity were observed than complex **2**. It is interesting to note, however, complex **1** showed lower cytotoxicity than complex **2** against four human tumor cell lines. Therefore, other biological targets other than DNA may be responsible for the in vitro cytotoxicity of the two zinc complexes.

Acknowledgments We thank the National Natural Science Foundation of China and the Natural Science Foundation for Colleges and Universities in Jiangsu province (07KJD320013) for financial supports.

References

- Berova N, Nakanishi K, Woody RW (2000) In circular dichroism: principles and applications, 2nd edn part II. Wiley, Chichester, p 748
- Choi C-F, Tsang P-T, Huang J-D, Chan EYM, Ko W-H, Fong W-P et al (2004) Synthesis and in vitro photodynamic activity of new hexadeca-carboxy phthalocyanines. *Chem Commun (Camb)* 2236–2237. doi:10.1039/b405868b
- Glover PB, Ashton PR, Childs LJ, Rodger A, Kercher M, Williams RM et al (2003) Hairpin-shaped heterometallic luminescent lanthanide complexes for dna intercalative recognition. *J Am Chem Soc* 125:9918–9919. doi:10.1021/ja029886s
- Hannon MJ (2007) Supramolecular DNA recognition. *Chem Soc Rev* 36:280–295. doi:10.1039/b606046n
- Haq I, Ladbury J (2000) Drug-DNA recognition: energetics and implications for design. *J Mol Recognit* 13:188–197. doi:10.1002/1099-1352(200007/08)13:4<;188::AID-JMR503>3.0.CO;2-I
- Harvey MA, Baggio S, Iban ez A, Baggio R (2004) Three zinc(II) complexes presenting a ZnN6 chromophore and with peroxodisulfate as the counter-ion. *Acta Cryst C60*:m375–m381
- Holder A, Swavey S, Brewer KJ (2004) Design aspects for the development of mixed-metal supramolecular complexes capable of visible light induced photocleavage of DNA. *Inorg Chem* 43:303–308. doi:10.1021/ic035029t
- Jiang Q, Xiao N, Shi P, Zhu Y, Guo Z (2007) Design of artificial metallonucleases with oxidative mechanism. *Coord Chem Rev* 251:1951–1972. doi:10.1016/j.ccr.2007.02.013
- Jiang Q, Wu Z, Zhang Y, Hotze ACG, Hannon MJ, Guo Z (2008) Effect of adenine moiety on DNA binding property of copper(II)–terpyridine complexes. *Dalton Trans* 3054–3060. doi:10.1039/b719010g
- Johansson O, Borgstroem M, Lomoth R, Palmblad M, Bergquist J, Hammarstroem L et al (2003) Electron donor–acceptor dyads based on ruthenium(II) bipyridine and terpyridine complexes bound to naphthalenediimide. *Inorg Chem* 42:2908–2918. doi:10.1021/ic020420k
- Juranović I, Meić Z, Piantanida I, Tumir L-M, Žinić M (2002) Interactions of phenanthridinium–nucleobase conjugates with polynucleotides in aqueous media. Recognition of poly U. *Chem Commun (Camb)* 1432–1433. doi:10.1039/b202615e
- Kovala-Demertzi D, Yadav PN, Wiecek J, Skoulika S, Varadinova T, Demertzis MA (2006) Zinc(II) complexes derived from pyridine-2-carbaldehyde thiosemicarbazone and (1E)-1-pyridin-2-ylethan-1-one thiosemicarbazone. Synthesis, crystal structures and antiproliferative activity of zinc(II) complexes. *J Inorg Biochem* 100:1558–1567. doi:10.1016/j.jinorgbio.2006.05.006
- Levine LA, Morgan CM, Ohr K, Williams ME (2005) Tetra-platinated artificial oligopeptides afford high affinity

- intercalation into dsDNA. *J Am Chem Soc* 127:16764–16765. doi:[10.1021/ja055162f](https://doi.org/10.1021/ja055162f)
- Li CK-L, Sun RW-Y, Kui SC-F, Zhu N, Che C-M (2006) Anticancer cyclometalated [AuIII π ACHTUNGTRUNG(C^NC)mL] n +compounds: synthesis and cytotoxic properties. *Chem Eur J* 12:5253–5266. doi:[10.1002/chem.200600117](https://doi.org/10.1002/chem.200600117)
- Martelli A, Constant J-F, Demeunynck M, Lhomme J, Dumy P (2002) Design of site specific DNA damaging agents for generation of multiply damaged sites. *Tetrahedron* 58:4291–4298. doi:[10.1016/S0040-4020\(02\)00345-9](https://doi.org/10.1016/S0040-4020(02)00345-9)
- Nejedlý K, Chládková J, Vorlíčková M, Hrabcová I, Kyr J (2005) Mapping the B-A conformational transition along plasmid DNA. *Nucleic Acids Res* 33(1):e5. doi:[10.1093/nar/gni008](https://doi.org/10.1093/nar/gni008)
- Neve F, Crispini A, Campagna S, Serroni S (1999) Synthesis, structure, photophysical properties, and redox behavior of cyclometalated complexes of iridium(III) with functionalized 2, 2'-bipyridines. *Inorg Chem* 38:2250–2258. doi:[10.1021/ic981308i](https://doi.org/10.1021/ic981308i)
- Novakova O, Kasparkova J, Vrana O, van Vliet PM, Reedijk J, Brabec V (1995) Correlation between cytotoxicity and DNA binding of polypyridyl ruthenium complexes. *Biochemistry* 34:12369–12378. doi:[10.1021/bi00038a034](https://doi.org/10.1021/bi00038a034)
- Sheldrick GM (1997) SHELX-97, A computer program for crystal structure solution and refinement. University of Göttingen (Germany)
- Sheldrick GM (2001) SADABS, Version 2, Multi-Scan absorption correction program. University of Göttingen (Germany)
- Shi P, Jiang Q, Zhao Y, Zhang Y, Lin J, Lin L et al (2006) DNA binding properties of novel cytotoxic gold(III) complexes of terpyridine ligands: the impact of steric and electrostatic effects. *J Biol Inorg Chem* 11:745–752. doi:[10.1007/s00775-006-0120-y](https://doi.org/10.1007/s00775-006-0120-y)
- Srivatsan SG, Parvez M, Verma S (2002) Modeling prebiotic catalysis with adenylated polymeric templates: crystal structure studies and kinetic characterization of template-assisted phosphate ester hydrolysis. *Chem Eur J* 8:5184. doi:[10.1002/1521-3765\(20021115\)8:22<5184::AID-CHEM5184>3.0.CO;2-2](https://doi.org/10.1002/1521-3765(20021115)8:22<5184::AID-CHEM5184>3.0.CO;2-2)
- Steiner T (1996) C–H...O hydrogen bonding in crystals. *Crystallogr Rev* 6:1–57. doi:[10.1080/08893119608035394](https://doi.org/10.1080/08893119608035394)
- Szaciłowski K, Macyk W, Drzewiecka-Matuszek A, Brindell M, Stochel G (2005) Bioinorganic photochemistry: frontiers and mechanisms. *Chem Rev* 105:2647–2694. doi:[10.1021/cr030707e](https://doi.org/10.1021/cr030707e)
- Tumir L-M, Piantanida I, Juranović Cindrić I, Hrenar T, Meićand Z, Žinić M (2003) New permanently charged phenanthridinium–nucleobase conjugates. Interactions with nucleotides and polynucleotides and recognition of ds-polyA₁₂. *J Phys Org Chem* 16:891–899. doi:[10.1002/poc.680](https://doi.org/10.1002/poc.680)
- Tumir L-M, Piantanida I, Juranović I, Meić Z, Tomić S, Žinić M (2005) Recognition of homo-polynucleotides containing adenine by a phenanthridinium bis-uracil conjugate in aqueous media. *Chem Commun (Camb)* 2561–2563. doi:[10.1039/b500617a](https://doi.org/10.1039/b500617a)